ELSEVIER

Journal of Crystal Growth 147 (1995) 326–332

JOURNAL OF CRYSTAL GROWTH

Effect of multilayered SrS–SrS:Ce–SrS phosphor prepared by multi-source deposition method on the thin film electroluminescent devices

Y.H. Lee [a,*], D.H. Kim [a,1], B.K. Ju [a], T.H. Yeom [a,2], T. S Hahn [a], M.H. Oh [a], S.H. Choh [b]

[a] *Division of Electronics and Information Technology, Korea Institute of Science and Technology, P.O. Box 131, Cheongryang, Seoul 136-701, South Korea*

[b] *Department of Physics, Korea University, Seoul 136-701, South Korea*

Received 17 June 1994; manuscript received in final form 20 October 1994

Abstract

Single-layer SrS:Ce and multilayer SrS–SrS:Ce–SrS thin films have been grown by multi-source deposition method. The X-ray diffraction patterns of the films showed the typical diffraction patterns of the cubic SrS powder. Single-layer SrS:Ce thin films exhibited sulfur deficiency and their fluorescence spectra showed a broad red emission peak. The multilayer SrS–SrS:Ce–SrS electroluminescent device showed nearly stoichiometric composition and an electroluminescent device made of these layers displayed a green-emission intensified spectrum with peaks located at 493 and 523 nm. A distinct S-shaped pinching effect in the transferred charge versus applied voltage characteristics, similar to a hysteretic electroluminescent device, was observed in multilayer device. We interpret that the separation of the light-emitting SrS:Ce layer from the two interfacial SrS layers and the resulting nonuniform space charge in the middle SrS:Ce layer are responsible for the observed enhancement of luminance through the intensified hysteretic effect in the multilayer structure.

1. Introduction

Since SrS:CeF_3 films were found to emit a bright greenish blue emission by Barrow et al., alkaline-earth sulfide phosphor films have been investigated intensively [1–4]. In recent studies, the development of an efficient blue phosphor is concentrated on the implementation of the efficiency improvement through multilayered phosphor structure. The basic concepts in this research are summarized as follows: (1) the crystalliny improvement of the main phosphor layer by assistance of good crystalline underlayer and (2) a large amount of carrier generation for the electroluminescence (EL) process. As previously shown by Mauch et al., the introduction of ZnS/SrS:Ce multilayered phosphors from 3 to 9 layers

* Corresponding author.

[1] Present address: Department of Physics, Yeungnam University, Kyungsan 712-749, South Korea.

[2] Present address: Department of Physics, Seonam University, Namwon, Junbuk 590-170, South Korea.

SSDI 0022-0248(94)00662-8

in a thin film electroluminescent device (TFELD) led to a remarkable improvement of luminance and efficiency [3,4]. The pure blue component luminance was found to exceed 10 cd/m^2 at 60 Hz. They suggest that the mechanisms leading to an improved performance are related to the enhancement of the trailing edge emission due to the additional interfaces in the multilayer case. On the other hand, Tsujiyama et al. [5] have reported a hysteretic effect in the blue-light emitting electroluminescent device with ZnS–SrS:Ce–ZnS structure. Hysteresis in the luminance (L) versus applied voltage (V) curve has also been reported in other studies [6,7].

In this paper, we prepared TFELDs consisting of a multilayered SrS–SrS:Ce–SrS phosphor structure using a multi-source deposition (MSD) system with a load-lock chamber. Crystallinity, composition profile, doping of emission centers, and type of the defect centers were examined by X-ray diffraction, Auger electron spectroscopy (AES), secondary ion mass spectrometry (SIMS), fluorescence spectroscopy, and electron paramagnetic resonance (EPR) to study the effect of separation of the carrier-generation layer from the light-emitting layer on the TFELD performance. Transferred charge versus applied voltage and conduction current versus applied voltage were also measured to evaluate the influence of the multilayer phosphors on the EL process.

2. Experiment

The samples were fabricated using a multi-source deposition system with a load-lock chamber, as shown in Fig. 1. The system was equipped with Sr, S, and $CeCl_3$ sources in pyrolytic boron nitride (PBN) crucibles heated by tantalum heaters. The process chamber was evacuated by a cryo-pump and a turbo-molecular pump down to the order of 10^{-8} Torr. After one processing cycle the base pressure was fixed by the outgassing of sulfur from the chamber walls. Evaporation rates of the sources were controlled by the temperature of the PBN crucibles. Sulfur powder was evaporated at about 110–120°C and the source temperatures of Sr and $CeCl_3$ were fixed at 590 and 650°C, respectively. The deposition rate of sulfur was difficult to control and the vacuum was about 5×10^{-5} Torr during the evaporation. Both single layer SrS:Ce films (#1) and multilayer SrS–SrS:Ce–SrS films (#2) were deposited on ITO-coated Corning 7059 glass substrates heated at 350°C. The shutter for $CeCl_3$ was controlled to grow the multilayer structures. A light-emitting SrS:Ce layer was formed after the deposition of a 70 nm thick SrS layer. After SrS:Ce layer formation, additional 70 nm thick SrS layer was deposited. The insulating Si_xN_y layer of 300 nm thickness was RF magnetron sputtered on top of the multilayer in the load-lock

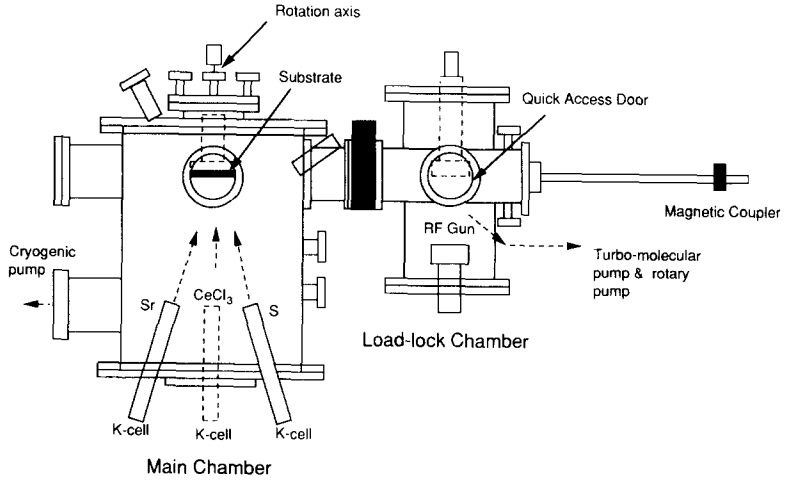

Fig. 1. Schematic diagram of the multi-source deposition system with load-lock chamber.

chamber without breaking the vacuum. We could, in this way, avoid any possible contamination from exposing to the air.

No post-deposition annealing was performed because annealing right after the deposition of the SrS–SrS:Ce–SrS film in the main chamber resulted in the appearance of bubbles in the film. This is probably due to the boiling of sulfur in our slightly sulfur-excess films. If this is the case, a high temperature annealing of any sulfur-excess SrS films may degrade the film quality due to the low boiling point of sulfur (440°C).

The fluorescence spectra of the sample #1 were measured at room temperature using a 150 W xenon-arc lamp (Osram XBO) for emission and excitation source. The stoichiometry of the specimens was determined by AES spectrometer (Perkin-Elmer ϕ 670). EPR experiments were performed to study the nature of the defect centers in the films. Bruker X-band EPR spectrometer (ESP 300) with TE_{102} rectangular cavity was used. The operating characteristics of the EL devices were measured using a Sawyer–Tower circuit and a modified Chen–Krupka circuit.

3. Results

X-ray diffraction patterns for the single (#1) and multilayer films (#2) showed that both films were well crystallized in the (200) orientation of NaCl structure as shown in Fig. 2. However, the full width at half maximum (FWHM) of the (200) peak of the SrS–SrS:Ce–SrS multilayer film was narrower than that of sample #1.

AES spectra after removing the surface layers by Ar sputtering are shown in Fig. 3a for sample #1 and in Fig. 3b for sample #2. Sample #1 shows sulfur deficiency, but sample #2 shows slight sulfur excess across the whole depth profile. It can be seen clearly that the oxygen contamination was suppressed by our MSD method even in the sulfur deficient sample #1. The activator element Ce was not followed during the depth profiles in order to reduce the measuring time. Instead, SIMS experiment was performed to ascertain the location of the Ce activators in #2. The result is shown in Fig. 3b. It is clear that Ce ions are positioned in the middle of the multilayer structure. Also note that the concentration of Ce is less than 1% of the Sr concentration.

We measured the fluoresence spectra of a sulfur-deficient SrS thin film. A strong and broad red fluorescence emission peak was observed in addition to the weak greenish blue peak. This red peak probably originates from defect centers [8]. The AES results indicate that these defects could be color centers associated with the sulfur vacancies.

In order to improve the stoichiometry of the

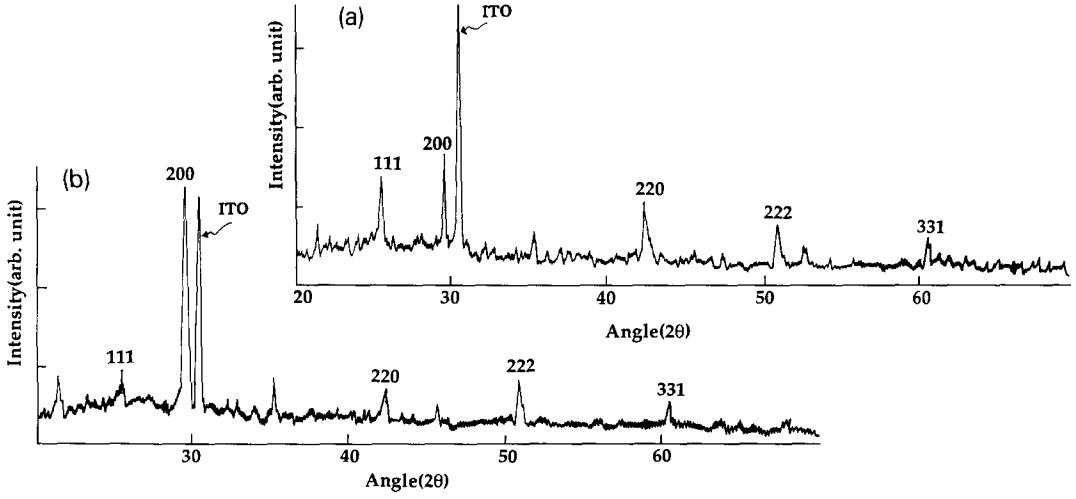

Fig. 2. X-ray diffraction patterns of (a) film #1 and (b) film #2 prepared by MSD with separate Sr, S, and $CeCl_3$ sources.

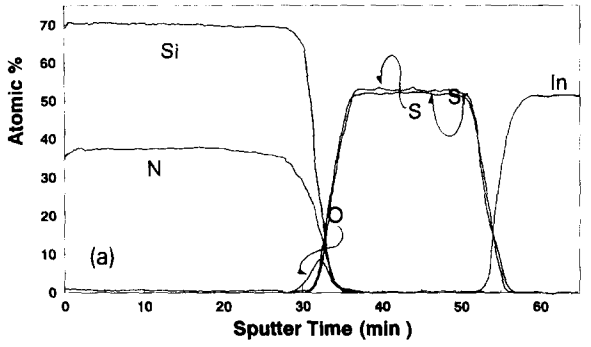

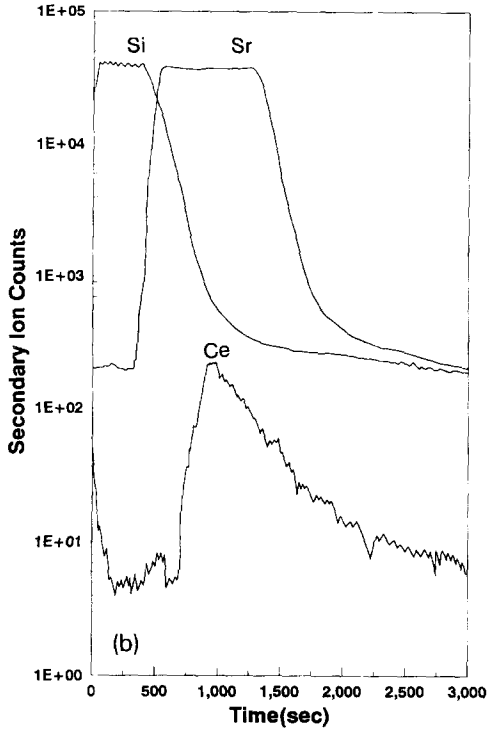

Fig. 3. (a) In-depth profiles of the composing ion concentration of structures #1 and #2 measured by AES. (b) Depth profile of Sr and Ce ions in SrS–SrS:Ce–SrS layered structure measured by SIMS using oxygen as primary ion source.

multilayer film, sufficient sulfur was intentionally evaporated. The EL spectrum of sulfur-excess SrS–SrS:Ce–SrS (#2) is blue-green, as shown in Fig. 4. Generally, two emission bands [9] have been observed in the luminescent spectrum of SrS:Ce. The 4f ground state of the Ce^{3+} ion splits into $^2F_{7/2}$ and $^2F_{5/2}$ states in the Russel–Saunders coupling approximation. The crystal field removes the degeneracy of these states only

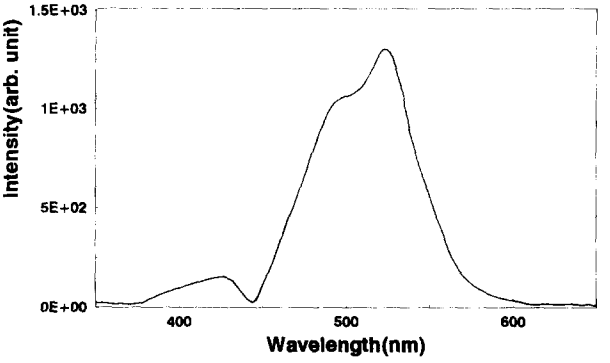

Fig. 4. Electroluminescence emission spectra of SrS–SrS:Ce–SrS TFELD.

very slightly, since the 4f orbital is well screened in the Ce^{3+} ion. On the other hand, the 5d orbital is strongly influenced by the O_h crystal field, so that it is split into widely separated e_g and t_{2g} states. The observed emission peaks are due to the transition from the lowest excited state $t_{2g}(5d)$ to $^2F_{7/2}$ and $^2F_{5/2}$ levels.

In the EPR experiment, as shown in Fig. 5, a symmetric resonance peak from F-centers was found in the sulfur-excess film #2. In our previous study [10], an F-center resonance peak was observed in sulfur deficient ZnS:Tb,F films [4]. However, the F-center was not detected by EPR in #1, although AES in-depth profiling in Fig. 3a showed overall sulfur deficiency. There are two

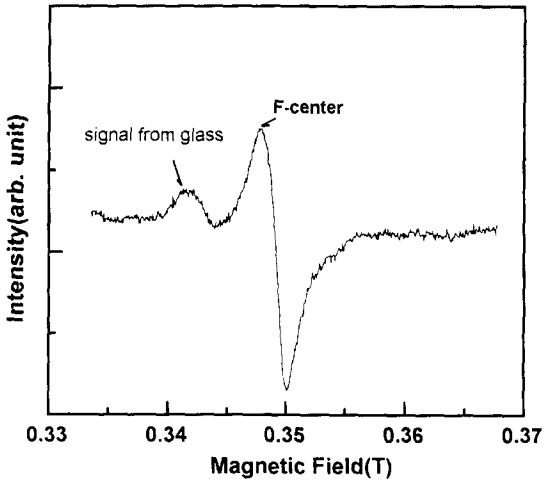

Fig. 5. Electron paramagnetic resonance spectra of film #2. One symmetric resonance signal observed.

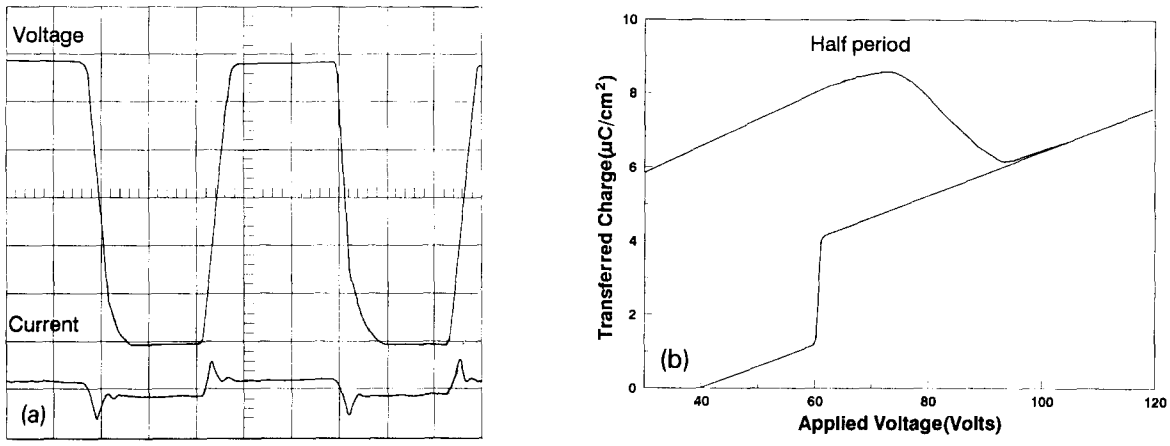

Fig. 6. (a) Current response versus applied voltage waveform. (b) Corresponding transferred charge versus applied voltage diagram.

well-known models of the F-center [11,12]. The vacancy model views that the F-center consists of an electron trapped in the field of a negative ion vacancy. The interstitial model, on the other hand, assumes that the F-center consists of an electron trapped in the field of an interstitial ion; it is thus an interstitial atom. In this study, we propose that the F-center in our sulfur excess film (#2) would be one electron trapped interstitially. The line width of the F-center signal was about 22.3 gauss broader than that of the F-center in a ZnS/ZnSe crystal [12] and ZnS:Tb,F film. The obtained g value was 2.012.

Fig. 6 shows the current waveforms and corresponding transfered charge versus applied voltage (Q–V) curves of device #2. The current waveform shows the two peaks with a step due to dissipative current. The Q–V characteristics show the distinct S-shaped diagram, which has a larger operating-voltage margin above the threshold voltage compared to that of a normal single SrS:Ce layer device.

4. Discussion

It has been known that the EL spectrum of conventional SrS:Ce shows two peaks around 475 and 515 nm. In our sulfur excess TFELD, the emission peaks were found to lie within the spectral region of the typical SrS:Ce emission, but the intensity of the longer wavelength is larger than that of the shorter one as shown in Fig. 4. This observation is an opposite trend to that found with the conventional SrS:Ce layer. In sulfur excess films, polysulfur ions such as S_2^{2-} are created or the Ce^{3+} emission center is oxidized to Ce^{4+}. The partial existence of Ce^{4+} and polysulfur can drastically increase the Sr^{2+} lattice vacancy concentration, and thus the resultant lattice distortion can give rise to a pronounced influence on the crystal field. A modification of the inner shell transitions of Ce, due to such a distortion of the crystal field, can be a source of the unusual EL spectrum. On the other hand, the quantum optical effect can modify the EL spectrum [13]. Since the total thickness of the phosphor and the insulating layer is of the order of the wavelength of the emitted light and the thickness of each component is a fraction of that wavelength, the quantum optical effect can be an important factor.

The observation of the F-centers with a nearly-free unpaired electron in the sulfur-excess films suggests that the major bulk defects are of this type. The F-centers will then be an extra source of the conduction electrons in addition to the tunnel injection from the insulator–SrS interface. The good crystallinity of the SrS layer also helps to increase the carrier density via creation of the electron–hole pairs by enhancing the efficiency of the impact ionization of the SrS host.

The created holes are swept to the interface by the electric field with or without filling the defects, but the created electrons easily become conduction electrons.

When the carriers are accelerated, the good crystallinity now helps to reduce the chance of collision for the carriers with the imperfections until reaching the SrS:Ce layer. The multi-slope characteristics of the Q–V curves (see Fig. 6b) are considered to be related to the effective ionization [14] of the middle SrS:Ce luminescent layer by the accelerated carriers under very high electric field (> 2 MV/cm), which is higher than the turn-on field (0.5–0.7 MV/cm). Both high carrier density and a nearly loss-free acceleration are supposed to be among the reasons for the high brightness of our device #2.

We next discuss the effect of the middle-positioned SrS:Ce layer on device operation in terms of hysteretic effect due to significantly nonuniform space-charge distribution. Hysteretic behavior was found in Q–V and L–V characteristics as shown in Figs. 6b and 7a, respectively. From the non-linear pinching at short side of the parallelogram of the Q–V diagram, it is suspected that the hysteretic mechanism for the device #2 would be similar to that of the hysteretic ZnS:Mn device [15,16]. A recent analytical model [17] for the typical hysteretic ZnS:Mn ELD that shows high luminance under low voltage driving strongly asserted that there exists a nonuniform distribution of space charge along the whole phosphor layer. The consequent electric field distribution, i.e. enhancement of the slope of the band bending, was necessary to explain the S-shaped Q–V (so-called hysteresis) properties.

The above analysis can be extended to our multilayer ELD. When an electric field is applied, shallow and deep traps in the front SrS layer release electrons. Those released electrons undergo a field assisted tunneling to the empty excited states of the Ce or Ce-related trap complexes [18] in the middle SrS:Ce layer, and ionize them. Under the same electric field, the electrons from the ionized Ce centers will be promoted to the conduction band due to the strong electric field originating from the band offset between the front, highly resistive undoped SrS and much less resistive Ce-doped SrS:Ce layer. Meanwhile electrons from the trap complexes will recombine with some of the holes created in the SrS:Ce layer by the impact ionization. Those instaneously trapped holes are now spatially frozen at the location of their creation, thereby inducing a space charge and subsequent distortion of the electric field distribution. While the applied field is sustained, the space-charge induced distortion of the electric field will persist.

The intentional separation of the SrS:Ce layer from undoped interfacial SrS layers in SrS–SrS:Ce–SrS structure encourages the development of a nonuniform space charge, thus inducing a large hysteresis in Q–V curves. According to Neyts [17], the large hysteresis is closely re-

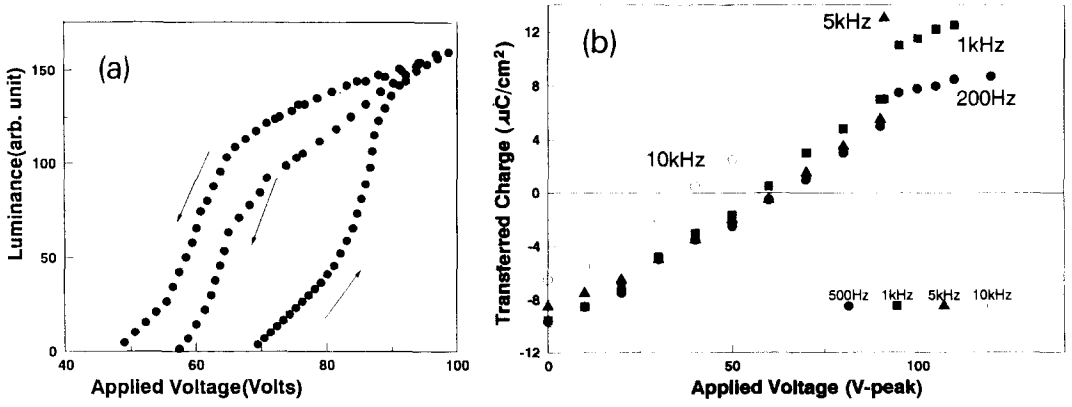

Fig. 7. (a) Luminance versus applied voltage curve. Distinct hysteresis was observed. However, after several hours of operation, hysteresis seemed to disappear. (b) Frequency dependence of Q–V shape for SrS–SrS:Ce–SrS TFELD.

lated to the high brightness. If we assume the presence of the concentrated space charge near the center of the whole phosphor structure, our Q–V characteristics and the high brightness of our device, in spite of very thin phosphor layer, are well matched to Neyts's simulation result. Also, the weakning of the distinct S-shaped Q–V diagram with the increase of the applied frequency as shown in Fig. 7b is a strong indication that the loss of the deeply trapped holes occurs predominantly through the recombination with the injected electrons.

5. Conclusion

Stoichiometric SrS films with good crystallinity can be grown by multi-source deposition method with a high level of control over the dopant concentration. A TFEL device with the unique multilayered SrS–SrS:Ce–SrS structure showed bright green-blue emission peaks corresponding to the typical transitions of Ce in SrS crystal field. It was suggested that the high luminance, in spite of very thin phosphor layer, resulted from (1) the effective excitation and/or ionization of SrS:Ce luminescent layer by the almost low loss acceleration of the hot carriers, due to the good crystallinity of the SrS layer, and (2) the distorted electric field in the SrS:Ce layer due to space charge formation by the trapped hole in the deep trap states associated with Ce emission center and consequent intensified hysteretic effect. The separation of the light-emitting SrS:Ce layer from the two interfacial SrS layers encourages the formation of nonuniform space charge in the middle SrS:Ce layer.

Acknowledgments

We would like to thank Y. Lee and S.G. Kim for the technical assistance in building the control unit for the MSD system. The cooperation by B.Y. Yu during the fluorescence experiments is gratefully acknowledged. This work has been supported by the Ministry of Science and Technology in Korea.

References

[1] W.A. Barrow, R.E. Coovert and C.N. King, in: Tech. Digest SID 84 (Society for Information Display) (1984) p. 249.
[2] S. Takana, V. Shanker, M. Shiiki, H. Deguchi and H. Kobayashi, in: Tech. Digest SID 85 (1985) p. 218.
[3] R.H. Mauch, K.O. Velthaus, H.W. Schock, S. Tanaka and H. Kobayashi, in: Tech. Digest SID 92 (1992) p. 178.
[4] R.H. Mauch, K.O. Velthaus, B. Huttl and H.W. Schock, in: Tech. Digest SID 93 (1993) p. 769.
[5] B. Tsujiyama, Y. Tamura, J. Ohwaki and H. Kozawaguchi, in: Tech. Digest SID 86 (1986) p. 37.
[6] K. Okamoto and K. Hanooka, Jap. J. Appl. Phys. 27 (1988) L 1923.
[7] S. Tanaka, H. Deguchi, Y. Mikami, M. Shiiki and H. Kobayashi, in: Tech. Digest SID 86 (1986) p. 29.
[8] D. Poelman, R.L. Van Meirhaeghe, W.H. Laflere and F. Cardon, J. Luminescence 52 (1992) 259.
[9] S. Tanaka, A. Miyakoshi and T. Nire, Electroluminescence, Springer Proc. in Physics (Springer, Berlin, 1989) p. 180.
[10] Y.H. Lee, B.K. Ju, T.H. Yeom, D.H. Kim, T.S. Hahn, M.H. Oh and S.H. Choh, to be submitted.
[11] B.S. Gourary and F.J. Adrian, Phys. Rev. 105 (1956) 1180.
[12] J. Scheides and A. Rauder, Solid State Commun. 5 (1967) 779.
[13] F. Williams, J. Luminescence 23 (1981) 1.
[14] S. Tanaka, K. Ohmi, K. Fujimoto, H. Kobayashi, T. Nire, A. Matsuno and A. Miyakoshi, in: Conf. Proc. Eurodisplay 93, EL-5 (1993) p. 237.
[15] W.E. Howard, O. Sahni and P.M. Alt, J. Appl. Phys. 53 (1982) 639.
[16] V. Marrello and A. Onton, IEEE Trans. Electron Devices ED-27 (1980) 1767.
[17] K.A. Neyts, IEEE Trans. Electron Devices ED-38 (1991) 2604.
[18] R.S. Crandall, M. Ling, J. Kane and P.N. Yocom, in: Tech. Digest SID 87 (1987) p. 245.
[19] S. Tanaka, H. Yoshiyama, Y. Mikami, J. Nishiura, S. Ohshio and H. Kobayashi, Proc. SID 29 (1988) 77.